SI Appendix

Stochastic reaction networks in dynamic compartment populations

Lorenzo Duso and Christoph Zechner

S.1 Modeling chemical reactions as transition classes

This section elaborates on the modeling of single-compartment chemical events as transition classes. Namely, we consider a stoichiometric equation of the form

$$u_{l,1}X_1 + \ldots + u_{l,D}X_D \xrightarrow{\tilde{h}_l(\mathbf{x})} v_{l,1}X_1 + \ldots + v_{l,D}X_D, \tag{S.1.1}$$

which can act on the content of each compartment in the population. We assume that the propensity function $\tilde{h}_l$ obeys mass-action kinetics

$$\tilde{h}_l(\mathbf{x}) = k_l \prod_{i=1}^{D} \binom{x_i}{u_{l,i}} = k_l g_l(\mathbf{x}) \tag{S.1.2}$$

with $k_l > 0$ being the rate constant for the reaction S.1.1, which is indexed by l. Whenever the reaction l occurs in a compartment of the population, the associated content $\mathbf{x}$ is updated by the change vector $\Delta\mathbf{x}_l = \mathbf{v}_l - \mathbf{u}_l$, with $\mathbf{u}_l = (u_{l,1}, \ldots, u_{l,D})$ and $\mathbf{v}_l = (v_{l,1}, \ldots, v_{l,D})$. From the compartment population perspective, the occurrence of one chemical reaction l in a single compartment of content $\mathbf{x}$ can be understood as an update of the population state $\mathbf{n}$ where $n(\mathbf{x})$ is decreased by 1 and $n(\mathbf{x} + \Delta\mathbf{x}_l)$ is increased by 1. The propensity function of such transition is given by the reaction propensity $\tilde{h}_l(\mathbf{x})$ times the factor $w(\mathbf{n}) = n(\mathbf{x})$, which is the number of compartments with content $\mathbf{x}$ in which the reaction could occur. Therefore, the stoichiometric equation S.1.1 corresponds to the transition class

$$[\mathbf{x}] \xrightarrow{h_l(\mathbf{n};\mathbf{x})} [\mathbf{y}], \qquad h_l(\mathbf{n};\mathbf{x},\mathbf{y}) = k_l g_l(\mathbf{x}) n(\mathbf{x}) \delta_{\mathbf{y},\mathbf{x}+\Delta\mathbf{x}_l}, \tag{S.1.3}$$

where the product-compartment distribution is a Kronecker delta that accounts for a change in $\mathbf{x}$ by the state-change vector $\Delta\mathbf{x}_l$. This transition class can be equivalently expressed in the more compact form

$$[\mathbf{x}] \xrightarrow{h_l(\mathbf{n};\mathbf{x})} [\mathbf{x} + \Delta\mathbf{x}_l], \qquad h_l(\mathbf{n};\mathbf{x}) = k_l g_l(\mathbf{x}) n(\mathbf{x}). \tag{S.1.4}$$

We remark that the rate constant k_l and the content dependent function $g_l(\mathbf{x})$ of the transition class S.1.3 simply correspond to the single-compartment mass-action propensity defined in eq. S.1.2. Furthermore, it is worth to emphasize that S.1.3 conserves the number of compartments in the population, consistently with our definition of chemical events. In summary, this shows how conventional stoichiometric equations of the form S.1.1 can be included in a compartment population model in terms of transition classes S.1.3.

S.2 Implementation of stochastic simulations

Across the case studies we have evaluated the accuracy of our moment-based approach by comparison with Monte Carlo averages obtained from exact stochastic simulations. In this section, we provide details about the efficient implementation of stochastic simulations for compartment population models.

We recall that the next-event waiting time distribution and next-event class distribution are determined by the value of the total class propensities $H_c(\mathbf{n})$, which are associated with the current state $\mathbf{n}$. For all classes c admitting self-contained moment dynamics, the total class

www.pnas.org/cgi/doi/10.1073/pnas.2003734117

propensities $H_c(\mathbf{n})$ are functions of some population moments. We denote by $\mathcal{M}$ the set of population moments that enter in the total class propensities $H_c(\mathbf{n})$, $c \in \mathcal{C}$, with $\mathcal{C}$ being the set of transition classes defining the population dynamics.

A stochastic simulation with initial condition $\mathbf{n}_0$ until time t_{max} proceeds as follows:

1. Set $t \leftarrow 0$ and $\mathbf{n} \leftarrow \mathbf{n}_0$
2. Compute the moments $\mathcal{M}(\mathbf{n})$
3. Compute $H_c \leftarrow H_c(\mathcal{M})$, $\forall c \in \mathcal{C}$, and $H_{TOT} \leftarrow \sum_c H_c$
4. Draw the next-event time as $t \leftarrow t + \left(-\frac{1}{H_{TOT}} \log(1-U)\right)$, with $U \sim \text{Uniform}[0,1)$
5. If $t < t_{max}$,
   draw the next-event class c^* from the discrete distribution $P(c^* = c) = \frac{H_c}{H_{TOT}}$
   else,
   end the simulation.
6. Draw the reactant compartments so that their contents $\mathbf{X}_{c^*}$ are sampled according to the distribution $h_{c^*}(\mathbf{n}; \mathbf{X}_{c^*})/H_{c^*}(\mathbf{n})$
7. When needed, draw the product compartments $\mathbf{Y}_{c^*}$ from $\pi_{c^*}(\mathbf{Y}_{c^*} \mid \mathbf{X}_{c^*})$
8. Update $\mathbf{n}$ and $\mathcal{M}$ according to the drawn transition, and go to 3

Note that the state of the system can be conveniently represented by storing the D-dimensional contents $\mathbf{x}_n$ of each compartment $n = 1, \ldots, N$ in a $D \times N$ integer matrix.

S.3 Derivation of the expected moment dynamics

Our goal is to derive the expected trajectory of the SDE

$$\mathrm{d}M^\gamma = \sum_{c \in \mathcal{C}} \sum_{j \in \mathcal{J}_c} \Delta M^\gamma_{c,j} \mathrm{d}R_{c,j}, \tag{S.3.5}$$

which describes the time evolution of an arbitrary population moment M^γ subject to a set $\mathcal{C}$ of transition classes. Using the Doob-Meyer decomposition theorem [1], we can decompose the differential reaction counter $\mathrm{d}R_{c,j}$ into a predictable part, related to its propensity function $h_{c,j}(\mathbf{n})$, and a martingale $Q_{c,j}$

$$\mathrm{d}R_{c,j} = h_{c,j}(\mathbf{n})\mathrm{d}t + \mathrm{d}Q_{c,j}. \tag{S.3.6}$$

We can substitute the decomposition S.3.6 into S.3.5 and take the expectation on both sides

$$\begin{aligned}
\mathrm{d}\langle M^\gamma \rangle &= \Big\langle \sum_{c \in \mathcal{C}} \sum_{j \in \mathcal{J}_c} \Delta M^\gamma_{c,j} (h_{c,j}(\mathbf{n})\mathrm{d}t + \mathrm{d}Q_{c,j}) \Big\rangle \\
&= \sum_{c \in \mathcal{C}} \sum_{j \in \mathcal{J}_c} \Delta M^\gamma_{c,j} \langle h_{c,j}(\mathbf{n})\mathrm{d}t + \mathrm{d}Q_{c,j} \rangle \\
&= \sum_{c \in \mathcal{C}} \sum_{j \in \mathcal{J}_c} \Delta M^\gamma_{c,j} \langle h_{c,j}(\mathbf{n}) \rangle \mathrm{d}t,
\end{aligned} \tag{S.3.7}$$

where the second term vanishes because of the martingale property of $Q_{c,j}$. Finally, since the moment update $\Delta M^\gamma_{c,j}$ is a constant for any fixed c and j, we can switch the order of summation and expectation in the last line of S.3.7 to obtain

$$\begin{aligned}
\frac{\mathrm{d}\langle M^\gamma \rangle}{\mathrm{d}t} &= \sum_{c \in \mathcal{C}} \sum_{j \in \mathcal{J}_c} \Delta M^\gamma_{c,j} \langle h_{c,j}(\mathbf{n}) \rangle \\
&= \sum_{c \in \mathcal{C}} \Big\langle \sum_{j \in \mathcal{J}_c} \Delta M^\gamma_{c,j} h_{c,j}(\mathbf{n}) \Big\rangle.
\end{aligned} \tag{S.3.8}$$

S.4 Conditions for self-contained moment dynamics

In this section we provide sufficient conditions for a transition class to yield moment dynamics whose r.h.s. depends exclusively on population moments. From eq. S.3.8 we observe that the contribution of class c to the expected dynamics of an arbitrary population moment M^γ is given by

$$\begin{aligned}\frac{\mathrm{d}\langle M^\gamma\rangle}{\mathrm{d}t} &= \Big\langle \sum_{j\in\mathcal{J}_c} \Delta M^\gamma_{c,j} h_{c,j}(\mathbf{n})\Big\rangle \\ &= \Big\langle \sum_{\mathbf{X}_c}\sum_{\mathbf{Y}_c} \Delta M^\gamma_c(\mathbf{X}_c,\mathbf{Y}_c) h_c(\mathbf{n};\mathbf{X}_c,\mathbf{Y}_c)\Big\rangle, \end{aligned} \tag{S.4.9}$$

where we have made explicit the reactant- and product- compartment contents $\mathbf{X}_c$ and $\mathbf{Y}_c$ involved in each specific instance $j=\varphi_c(\mathbf{X}_c,\mathbf{Y}_c)$ and accordingly parametrized the moment update and the propensity function. The sums over $\mathbf{X}_c$ and $\mathbf{Y}_c$ are thus intended to enumerate all distinguishable transitions of class c. If now we substitute the full expression of h_c into S.4.9 we obtain

$$\begin{aligned}\frac{\mathrm{d}\langle M^\gamma\rangle}{\mathrm{d}t} &= k_c\Big\langle \sum_{\mathbf{X}_c} w(\mathbf{n};\mathbf{X}_c) g_c(\mathbf{X}_c) \sum_{\mathbf{Y}_c} \Delta M^\gamma_c(\mathbf{X}_c,\mathbf{Y}_c)\pi_c(\mathbf{Y}_c\mid\mathbf{X}_c)\Big\rangle \\ &= k_c\Big\langle \sum_{\mathbf{X}_c} w(\mathbf{n};\mathbf{X}_c) g_c(\mathbf{X}_c) \langle \Delta M^\gamma_c(\mathbf{X}_c,\mathbf{Y}_c)\mid\mathbf{X}_c\rangle\Big\rangle, \end{aligned} \tag{S.4.10}$$

with $\langle\cdot\,|\,\mathbf{X}_c\rangle$ as the conditional expectation with respect to π_c. We recall that $\Delta M^\gamma_c(\mathbf{X}_c,\mathbf{Y}_c)$ is a polynomial in $\mathbf{X}_c$ and $\mathbf{Y}_c$ by construction, because it is defined as a difference of discrete compartment contents raised to non-negative, integer exponents γ. Thus, the expectation $\langle\Delta M^\gamma_c(\mathbf{X}_c,\mathbf{Y}_c)\mid\mathbf{X}_c\rangle$ will in general contain terms of the form $\langle\mathbf{Y}_c^{\boldsymbol{\xi}}\mid\mathbf{X}_c\rangle$ for some $\xi_i\le\gamma_i$, $i=1,\dots,D$, that is, the moments of the conditional distribution π_c up to order γ. Besides that, the combinatorial weight $w(\mathbf{n};\mathbf{X}_c)$ has been defined as a product of binomials, which implies that it is a polynomial in $n(\mathbf{x})$, for $\mathbf{x}\in\mathbf{X}_c$.

At this point we can see under which condition the sum over $\mathbf{X}_c$ will produce a function of some population moments on the right-hand side of S.4.10. What we need to require is that the product $g_c(\mathbf{X}_c)\langle\Delta M^\gamma_c(\mathbf{X}_c,\mathbf{Y}_c)\mid\mathbf{X}_c\rangle$ is a polynomial in $\mathbf{X}_c$: in that case, the sum over $\mathbf{X}_c$ next to the terms $n(\mathbf{x})$ will result in a function of population moments. Thus, $g_c(\mathbf{X}_c)\langle\Delta M^\gamma_c(\mathbf{X}_c,\mathbf{Y}_c)\mid\mathbf{X}_c\rangle$ being a polynomial is a sufficient condition for the propensity of class c to admit a self-contained form. For instance, this condition is satisfied if

- $g_c(\mathbf{X}_c)$ has polynomial dependency on $\mathbf{X}_c$, and
- the moments of $\pi_c(\mathbf{Y}_c\mid\mathbf{X}_c)$ are polynomials in $\mathbf{X}_c$,

since a product of polynomials is in turn a polynomial. This corresponds to the sufficient condition reported in the main text.

S.5 Ito's rule for counting processes

Starting from eq. S.3.5, a stochastic differential equation can be obtained also for functions of one or more population moments by means of Ito's rule for counting processes [2]. Considering a function $f(M^\gamma)$, its SDE is obtained as

$$\mathrm{d}f(M^\gamma) = \sum_{c\in\mathcal{C}}\sum_{j\in\mathcal{J}_c}\big[f\big(M^\gamma+\Delta M^\gamma_{c,j}\big)-f(M^\gamma)\big]\mathrm{d}R_{c,j}. \tag{S.5.11}$$

For instance, eq. S.5.11 can be used to evaluate the stochastic dynamics of the square $(M^\gamma)^2$ of a population moment. The SDE of a function of multiple population moments, such as the cross-product $f(M^{\gamma'},M^{\gamma''})=M^{\gamma'}M^{\gamma''}$, is obtained in a similar manner by evaluating the overall change before and after the transition. Importantly, the simultaneous update of both moments has to be taken into account when computing the change of $f(M^{\gamma'},M^{\gamma''})$.

S.6 Multivariate Gamma moment closure for compartment-population models

Similarly to all moment-based approaches, also our moment equation method for compartment-population dynamics usually requires the use of some moment closure approximation in order to obtain a finite set of ODEs. Moment closure is a technique that approximates all occurrences of moments higher than a certain order with functions of lower order moments within a set of moment equations. The accuracy of moment closure depends on the particular model under consideration as well as its parameters and initial condition [3].

For the purposes of our work, we require a multivariate closure scheme. We compared three established multivariate closures across our case studies, i.e., the normal, lognormal and Gamma closure. We found the Gamma closure proposed by [4] to consistently outperform the other two closures, which is why we adopted this choice for all our case studies. We generally consider second-order closures (i.e., replacing moments of order higher than two), unless stated differently. In particular, we applied the following Gamma closure schemes:

- Closing a third-order cross product between a moment M^γ and a moment M^ξ, with M^γ appearing to the second power

$$\langle (M^\gamma)^2 M^\xi \rangle = 2\frac{\langle (M^\gamma)^2 \rangle \langle M^\gamma M^\xi \rangle}{\langle M^\gamma \rangle} - \langle (M^\gamma)^2 \rangle \langle M^\xi \rangle. \tag{S.6.12}$$

- Closing a single moment appearing at order 3, e.g. $\langle M^3 \rangle = \sum_{x=0}^{\infty} x^3 \langle n(x) \rangle$

$$\langle M^3 \rangle = 2\frac{\langle M^2 \rangle^2}{\langle M^1 \rangle} - \frac{\langle M^1 \rangle \langle M^2 \rangle}{\langle N \rangle}. \tag{S.6.13}$$

  which is also a Gamma closure, but corrected with the fact that the expected content distribution $\langle n(x) \rangle$ has normalization equal to $\langle N \rangle$.

S.7 CASE STUDY: Nested birth-death process

The transition classes that define the first case study are given by

$$\begin{aligned}
\emptyset &\xrightarrow{h_I(\mathbf{n};y)} [y] && h_I(\mathbf{n};y) = k_I \pi_{Poiss}(y;\lambda) \\
[x] &\xrightarrow{h_E(\mathbf{n};x)} \emptyset && h_E(\mathbf{n};x) = k_E n(x) \\
[x] &\xrightarrow{h_b(\mathbf{n};x)} [x+1] && h_b(\mathbf{n};x) = k_b n(x) \\
[x] &\xrightarrow{h_d(\mathbf{n};x)} [x-1] && h_d(\mathbf{n};x) = k_d x n(x).
\end{aligned} \tag{S.7.14}$$

We proceed below with a step-by-step derivation of both SDE and moment equations for this model.

S.7.1 Moment equations

The expected trajectory for $\langle N \rangle$ is already reported in the main text. To characterize the dynamics of N^2, we consider again the SDE for N, which reads

$$\mathrm{d}N = \mathrm{d}\bar{R}_I - \mathrm{d}\bar{R}_E, \tag{S.7.15}$$

and we calculate the SDE for N^2 using Ito's rule for counting processes (eq. S.5.11)

$$\begin{aligned}
\mathrm{d}N^2 &= \left[(N+1)^2 - N^2\right]\mathrm{d}\bar{R}_I + \left[(N-1)^2 - N^2\right]\mathrm{d}\bar{R}_E \\
&= (1+2N)\mathrm{d}\bar{R}_I + (1-2N)\mathrm{d}\bar{R}_E.
\end{aligned} \tag{S.7.16}$$

The expectation of S.7.16 is

$$\frac{\mathrm{d}\langle N^2 \rangle}{\mathrm{d}t} = k_I(1 + 2\langle N \rangle) + k_E\big(\langle N \rangle - 2\langle N^2 \rangle\big). \tag{S.7.17}$$

We note that the evolution of $\langle N^2 \rangle$ is already in closed form. The SDE for the total mass M^1 includes also the contribution of the birth-death reactions taking place in each compartment, thus

$$\mathrm{d}M^1 = \sum_{y=0}^{\infty}(+y)\mathrm{d}R_{I,y} + \sum_{x=0}^{\infty}(-x)\mathrm{d}R_{E,x} + \sum_{x=0}^{\infty}(+1)\mathrm{d}R_{b,x} + \sum_{x=0}^{\infty}(-1)\mathrm{d}R_{d,x}. \tag{S.7.18}$$

Recalling that the content of newly created compartments is chosen to be Poisson distributed with parameter λ, the expected trajectory for the total mass is

$$\begin{aligned}\frac{\mathrm{d}\langle M^1\rangle}{\mathrm{d}t} &= k_I\Big\langle \sum_{y=0}^{\infty} y\pi_I(y;\lambda)\Big\rangle - k_E\Big\langle \sum_{x=0}^{\infty} xn(x)\Big\rangle + k_b\Big\langle \sum_{x=0}^{\infty} n(x)\Big\rangle - k_d\Big\langle \sum_{x=0}^{\infty} xn(x)\Big\rangle \\ &= k_I\lambda - k_E\langle M^1\rangle + k_b\langle N\rangle - k_d\langle M^1\rangle,\end{aligned} \tag{S.7.19}$$

as shown in the main paper. Similarly to N^2, we derive now the SDE for $(M^1)^2$ by Ito's rule

$$\begin{aligned}\mathrm{d}(M^1)^2 =& \sum_{y=0}^{\infty}\big[(M^1+y)^2 - (M^1)^2\big]\mathrm{d}R_{I,y} + \sum_{x=0}^{\infty}\big[(M^1-x)^2 - (M^1)^2\big]\mathrm{d}R_{E,x} \\ &+ \sum_{x=0}^{\infty}\big[(M^1+1)^2 - (M^1)^2\big]\mathrm{d}R_{b,x} + \sum_{x=0}^{\infty}\big[(M^1-1)^2 - (M^1)^2\big]\mathrm{d}R_{d,x} \\ =& \sum_{y=0}^{\infty}\big[y^2 + 2yM^1\big]\mathrm{d}R_{I,y} + \sum_{x=0}^{\infty}\big[x^2 - 2xM^1\big]\mathrm{d}R_{E,x} \\ &+ \sum_{x=0}^{\infty}\big[1 + 2M^1\big]\mathrm{d}R_{b,x} + \sum_{x=0}^{\infty}\big[1 - 2M^1\big]\mathrm{d}R_{d,x}.\end{aligned} \tag{S.7.20}$$

The expected trajectory for $\langle (M^1)^2\rangle$ equals

$$\begin{aligned}\frac{\mathrm{d}\langle (M^1)^2\rangle}{\mathrm{d}t} =& k_I\Big\langle \sum_{y=0}^{\infty}(y^2 + 2yM^1)\pi_I(y;\lambda)\Big\rangle + k_E\Big\langle \sum_{x=0}^{\infty}(x^2 - 2xM^1)n(x)\Big\rangle \\ &+ k_b\Big\langle \sum_{x=0}^{\infty}(1+2M^1)n(x)\Big\rangle + k_d\Big\langle \sum_{x=0}^{\infty}(1-2M^1)xn(x)\Big\rangle \\ =& k_I\lambda(1+\lambda+2\langle M^1\rangle) + k_E(\langle M^2\rangle - 2\langle (M^1)^2\rangle) \\ &+ k_b(\langle N\rangle + 2\langle NM^1\rangle) + k_d(\langle M^1\rangle - 2\langle (M^1)^2\rangle).\end{aligned} \tag{S.7.21}$$

This result introduces a dependency on two higher order moments, $\langle M^2\rangle$ and $\langle NM^1\rangle$. By observing that the expectation of eq. S.5.11 can be written as

$$\frac{\mathrm{d}\langle f(M^\gamma)\rangle}{\mathrm{d}t} = \sum_{c\in\mathcal{C}}\Big\langle \sum_{j\in\mathcal{J}_c}\big[f\big(M^\gamma + \Delta M^\gamma_{c,j}\big) - f(M^\gamma)\big]h_{c,j}(\mathbf{n})\Big\rangle, \tag{S.7.22}$$

we find respectively

$$\begin{aligned}\frac{\mathrm{d}\langle M^2\rangle}{\mathrm{d}t} =& k_I\Big\langle \sum_{y=0}^{\infty}(y^2)\pi_I(y;\lambda)\Big\rangle + k_E\Big\langle \sum_{x=0}^{\infty}(-x^2)n(x)\Big\rangle \\ &+ k_b\Big\langle \sum_{x=0}^{\infty}\big[(x+1)^2 - x^2\big]n(x)\Big\rangle + k_d\Big\langle \sum_{x=0}^{\infty}\big[(x-1)^2 - x^2\big]xn(x)\Big\rangle \\ =& k_I\lambda(1+\lambda) - k_E\langle M^2\rangle + k_b(\langle N\rangle + 2\langle M^1\rangle) + k_d(\langle M^1\rangle - 2\langle M^2\rangle)\end{aligned} \tag{S.7.23}$$

and

$$\begin{aligned}\frac{\mathrm{d}\langle NM^1\rangle}{\mathrm{d}t} &= k_I\Big\langle \sum_{y=0}^{\infty}\big[(N+1)(M^1+y)-NM^1\big]\pi_I(y;\lambda)\Big\rangle \\ &\quad + k_E\Big\langle \sum_{x=0}^{\infty}\big[(N-1)(M^1-x)-NM^1\big]n(x)\Big\rangle \\ &\quad + k_b\Big\langle \sum_{x=0}^{\infty}\big[(N(M^1+1)-NM^1\big]n(x)\Big\rangle \\ &\quad + k_d\Big\langle \sum_{x=0}^{\infty}\big[(N(M^1-1)-NM^1\big]xn(x)\Big\rangle \\ &= k_I\big(\lambda(1+\langle N\rangle)+\langle M^1\rangle\big)+k_E(\langle M^1\rangle-2\langle NM^1\rangle)+k_b\langle N^2\rangle-k_d\langle NM^1\rangle. \end{aligned} \tag{S.7.24}$$

Both eqs. S.7.23 and S.7.24 do not involve any higher-order moments. In summary, we obtained a closed system of 6 differential equations

$$\begin{aligned}\frac{\mathrm{d}\langle N\rangle}{\mathrm{d}t} &= k_I - k_E\langle N\rangle \\ \frac{\mathrm{d}\langle N^2\rangle}{\mathrm{d}t} &= k_I(1+2\langle N\rangle)+k_E\big(\langle N\rangle-2\langle N^2\rangle\big) \\ \frac{\mathrm{d}\langle M^1\rangle}{\mathrm{d}t} &= k_I\lambda - k_E\langle M^1\rangle + k_b\langle N\rangle - k_d\langle M^1\rangle \\ \frac{\mathrm{d}\langle (M^1)^2\rangle}{\mathrm{d}t} &= k_I\lambda(1+\lambda+2\langle M^1\rangle)+k_E(\langle M^2\rangle-2\langle (M^1)^2\rangle) \\ &\quad + k_b(\langle N\rangle+2\langle NM^1\rangle)+k_d(\langle M^1\rangle-2\langle (M^1)^2\rangle) \\ \frac{\mathrm{d}\langle M^2\rangle}{\mathrm{d}t} &= k_I\lambda(1+\lambda)-k_E\langle M^2\rangle+k_b(\langle N\rangle+2\langle M^1\rangle)+k_d(\langle M^1\rangle-2\langle M^2\rangle) \\ \frac{\mathrm{d}\langle NM^1\rangle}{\mathrm{d}t} &= k_I\big(\lambda(1+\langle N\rangle)+\langle M^1\rangle\big)+k_E(\langle M^1\rangle-2\langle NM^1\rangle)+k_b\langle N^2\rangle-k_d\langle NM^1\rangle. \end{aligned} \tag{S.7.25}$$

After numerical integration, the time evolution of the standard deviations for N and M^1 can be calculated by $\sqrt{\langle N^2\rangle-\langle N\rangle^2}$ and $\sqrt{\langle (M^1)^2\rangle-\langle M^1\rangle^2}$, respectively.

S.7.2 Simulation parameters

Figures 2B-C in the main paper have been generated using the following choice of parameters

$$k_I = 1 \qquad \lambda = 10 \qquad k_E = 0.01 \qquad k_b = 1 \qquad k_d = 0.1$$

and with initial condition

$$\mathbf{n}_0 : n_0(1) = 1,\ \ n_0(x) = 0\ \ \forall x \neq 1$$

which represents a population comprising one compartment with content $x = 1$. Monte Carlo estimates have been obtained by averaging the outputs of 10^3 stochastic simulations.

S.7.3 Steady-state moments

As already explained in the main paper, in this model the dynamics of the total number of compartments N is independent of the other moments of the system. This can be observed from the SDE S.7.15, which corresponds to the dynamics of a birth-death process with propensities $H_I(\mathbf{n}) = k_I$ and $H_E(\mathbf{n}) = k_E N$. This shall not be confused with the chemical birth-death process with propensities $\tilde{h}_b(x) = k_b$ and $\tilde{h}_d(x) = k_d x$, affecting the content x inside each compartment. Eq. S.7.15 implies that the steady state number of compartments N_∞ is Poisson distributed with mean k_I/k_E. This is resembled also by the steady-state solution of the moment equations, for which we find that $\langle N_\infty\rangle = k_I/k_E$ and $\langle N_\infty^2\rangle = k_I/k_E(1+k_I/k_E)$, so that

$$\mathrm{Var}(N_\infty) = \langle N_\infty^2\rangle - \langle N_\infty\rangle^2 = k_I/k_E = \langle N_\infty\rangle, \tag{S.7.26}$$

consistent with Poissonian noise. From the steady-state solution of the moment equations we can further derive the steady-state total mass

$$\langle M^1_\infty \rangle = \frac{k_b k_I/k_E + k_I \lambda}{k_d + k_E} = \frac{k_I}{k_E}\left[\frac{k_b}{k_d}\frac{1+\alpha\beta}{1+\alpha}\right] = \langle N_\infty \rangle \left[\frac{k_b}{k_d}\frac{1+\alpha\beta}{1+\alpha}\right], \tag{S.7.27}$$

where we introduced the dimensionless parameters $\alpha = k_E/k_d$ and $\beta = \lambda/(k_b/k_d)$. We notice that the term in square brackets in eq. S.7.27 represents the average steady-state content per compartment, which we denote by $\langle m_\infty \rangle = \langle M^1_\infty \rangle / \langle N_\infty \rangle$. In particular, $\langle m_\infty \rangle$ can be also interpreted as the mean value of the steady-state normalized expected distribution $P_\infty(x) = \langle n_\infty(x) \rangle / \langle N_\infty \rangle$, since

$$\langle m_\infty \rangle = \frac{\langle M^1_\infty \rangle}{\langle N_\infty \rangle} = \frac{\lim_{t\to\infty} \langle \sum_{x=0}^{\infty} x n(x) \rangle}{\langle N_\infty \rangle} = \sum_{x=0}^{\infty} x \frac{\langle n_\infty(x) \rangle}{\langle N_\infty \rangle} = \sum_{x=0}^{\infty} x P_\infty(x). \tag{S.7.28}$$

Similarly, it is possible to calculate $\langle M^2_\infty \rangle$ from the steady-state solution of the moment equations, and consequently identify the second order moment of $P_\infty(x)$ as

$$\langle s_\infty \rangle = \frac{\langle M^2_\infty \rangle}{\langle N_\infty \rangle} = \sum_{x=0}^{\infty} x^2 P_\infty(x). \tag{S.7.29}$$

After some algebraic manipulations, we can obtain the variance-to-mean ratio of $P_\infty(x)$ as

$$\begin{aligned} \frac{\sigma^2_\infty}{\langle m_\infty \rangle} &= \frac{\langle s_\infty \rangle - \langle m_\infty \rangle^2}{\langle m_\infty \rangle} = \frac{\sum_x x^2 P_\infty(x) - \left(\sum_x x P_\infty(x)\right)^2}{\langle m_\infty \rangle} \\ &= 1 + \frac{k_b}{k_d}\frac{\alpha}{(1+\alpha)(2+\alpha)}\frac{(\beta-1)^2}{1+\alpha\beta} \\ &= 1 + \langle m_\infty \rangle \frac{\alpha}{2+\alpha}\frac{(\beta-1)^2}{(1+\alpha\beta)^2}. \end{aligned} \tag{S.7.30}$$

An interesting insight from this result is that the variance-to-mean ratio achieves the minimum value 1 for $\beta = 1$. This indicates that the steady-state compartment content follows Poissonian statistics if $\lambda = k_b/k_d$, meaning that the content of compartments entering the system matches in distribution the chemical birth-death process occurring inside each compartment. Instead, whenever $\lambda \neq k_b/k_d$, the compartment content will have a limiting distribution with super-Poissonian noise.

S.7.4 Steady-state distribution

As mentioned in the main text, the expected number distribution $\langle n(x) \rangle$ is analytically intractable in most practical situations and our moment-based approach was conceived to address this problem. However, in the special case of the nested birth-death process, a treatment in terms of $\langle n(x) \rangle$ is straightforward since its transition classes have propensities which are linear in the compartment distribution $\mathbf{n}$. In the following, we show how a master equation for $\langle n(x) \rangle$ can be obtained directly from our counting process model, which is useful to demonstrate how our approach relates to the expected number distribution. Moreover, we provide analytical steady-state solutions for this master equation for two special parameter regimes.

The stochastic dynamics of $n(x)$ is given by

$$\mathrm{d}n(x) = \mathrm{d}R_{I,x} - \mathrm{d}R_{E,x} + \mathrm{d}R_{b,x-1} - \mathrm{d}R_{b,x} + \mathrm{d}R_{d,x+1} - \mathrm{d}R_{d,x}. \tag{S.7.31}$$

Note that the term $\mathrm{d}R_{b,x-1}$ is absent when $x = 0$. Similarly to the derivations in section S.3, we can make use of the Doob-Meyer decomposition and apply the expectation operator on both sides of S.7.31 to obtain an ordinary differential equation for the expected distribution $\langle n(x) \rangle$, which reads

$$\begin{aligned} \frac{\mathrm{d}\langle n(x) \rangle}{\mathrm{d}t} = & \underbrace{k_I \pi_I(x;\lambda) - k_E \langle n(x) \rangle}_{\text{compartment events}} \\ & + \underbrace{k_b\big(\langle n(x-1) \rangle - \langle n(x) \rangle\big) + k_d\big[(x+1)\langle n(x+1) \rangle - x\langle n(x) \rangle\big]}_{\text{chemical events}}. \end{aligned} \tag{S.7.32}$$

The terms in the second line are reminiscent of those obtained in a standard chemical master equation for a pure birth-death process, while those appearing in the first line account for compartmental dynamics. Note that $\langle n(x)\rangle$ obeys the special normalization $\sum_{x=0}^{\infty}\langle n(x)\rangle = \langle N\rangle$, with $\langle N\rangle$ as the expected number of compartments. At steady state, the left-hand side of eq. S.7.32 is zero, which yields the linear system of equations

$$k_I\pi_I(x;\lambda) + k_b\langle n_\infty(x-1)\rangle + k_d(x+1)\langle n_\infty(x+1)\rangle - (k_E + k_b + xk_d)\langle n_\infty(x)\rangle = 0 \quad \text{(S.7.33)}$$

for $x \in \mathbb{N}$, and

$$k_I\pi_I(0;\lambda) + k_d\langle n_\infty(1)\rangle - (k_E + k_b)\langle n_\infty(0)\rangle = 0 \quad \text{(S.7.34)}$$

for $x = 0$. Numerical solutions of this equation can be calculated in a straightforward manner by truncating the domain of x to a sufficiently large region and solving the resulting (finite) system of equations via matrix inversion. Moreover, simple closed-form expressions can be obtained for two special parameter configurations as described in the following.

We first introduce the generating function of the steady-state expected number distribution $G(z) = \sum_{x=0}^{\infty} z^x\langle n_\infty(x)\rangle$. An ordinary differential equation for $G(z)$ can be obtained by multiplying S.7.33 with z^x and summing over all x [5], which gives

$$k_d(1-z)G'(z) + [k_b(z-1) - k_E]G(z) + k_I e^{\lambda(z-1)} = 0, \quad \text{(S.7.35)}$$

with the special boundary condition $G(1) = \langle N_\infty\rangle$. The latter stems from the fact that the expected number distribution at steady state sums up to $\langle N_\infty\rangle$ (as opposed to one).

If we now set $\lambda = k_b/k_d$ (i.e. $\beta = 1$), the solution of S.7.35 is given by

$$G(z) = \frac{k_I}{k_E} e^{\frac{k_b}{k_d}(z-1)}, \quad \text{(S.7.36)}$$

which upon back-transformation yields

$$\langle n_\infty(x)\rangle = \langle N_\infty\rangle \frac{\lambda^x e^{-\lambda}}{x!} \quad \text{(S.7.37)}$$

with $\langle N_\infty\rangle = k_I/k_E$. Dividing S.7.37 by $\langle N_\infty\rangle$ reveals $P_\infty(x)$, in this case a Poisson distribution with mean $\lambda = k_b/k_d$.

Another interesting case where a simple closed-form solution of eq. S.7.35 can be found is when the degradation of molecules inside compartments is negligibly slow ($k_d = 0$). In this situation, new compartments are generated by the intake process and the birth reaction keeps producing new molecules in each compartment, until removed by the random exit process. By setting $k_d = 0$ in S.7.35 we find

$$G(z) = \frac{k_I}{k_E} e^{\lambda(z-1)} \frac{1}{1 - k_b(z-1)/k_E}. \quad \text{(S.7.38)}$$

Back-transformation of $G(z)$ yields for the stationary expected number distribution

$$\begin{aligned}\langle n_\infty(x)\rangle &= \langle N_\infty\rangle(1-\xi)\sum_{y=0}^{x}\xi^{x-y}\pi_{Poiss}(y;\lambda) \\ &= \langle N_\infty\rangle(1-\xi)\xi^x e^{\lambda(1/\xi-1)}\frac{\Gamma(1+x,\lambda/\xi)}{x!}, \end{aligned} \quad \text{(S.7.39)}$$

with $\xi = k_b/(k_b + k_E)$, Γ being the upper incomplete Gamma function and $\langle N_\infty\rangle = k_I/k_E$ as before. The solution S.7.39 can be also obtained by directly solving eq. S.7.33 recursively. The resulting distribution becomes more and more skewed as ξ increases (i.e. $k_b \gg k_E$), reflecting the fact that the birth process operates on average for a longer time span before the exit event occurs. In the case where newly arriving compartments are initially empty (i.e. λ=0), the distribution from S.7.39 simplifies to $\langle n_\infty(x)\rangle = \langle N_\infty\rangle(1-\xi)\xi^x$, which is a geometric distribution multiplied by the expected total number of compartments $\langle N_\infty\rangle$. As a consequence of the geometric distribution, $P_\infty(x) = (1-\xi)\xi^x$ can be interpreted as the probability for a single compartment to produce x molecules before exiting the system. Thus, the parameter ξ represents the "success probability" for the next event of a specific compartment to be a birth reaction. Conversely, the factor $(1-\xi)$ represents the probability that the next event is the compartment exit, which therefore ends the lifetime of the compartment in the population.

S.7.5 Analysis of total mass fluctuations and comparison with a static population

In this section we aim to study the fluctuations of the total population mass. It is important to realize that this is different from the analysis provided in section S.7.3, which focused on the statistics of the steady-state expected number distribution $\langle n_\infty(x)\rangle$. We remark that $\langle n(x)\rangle$ is an expected quantity that neglects fluctuations across realizations of the compartment population. Correspondingly, its variance only represents the variability of the *expected* content across individual compartments. Instead, the total mass $M^1 = \sum_{x=0}^{\infty} xn(x)$ is a random variable dependent on the full stochastic state $\mathbf{n}$. Thus, its fluctuations are adequately described by the variance $\mathrm{Var}(M^1)$, i.e.

$$\mathrm{Var}(M^1) = \langle (M^1)^2\rangle - \langle M^1\rangle^2 = \left\langle \left(\sum_{x=0}^{\infty} xn(x)\right)^2 \right\rangle - \left\langle \sum_{x=0}^{\infty} xn(x)\right\rangle^2. \tag{S.7.40}$$

In order to better highlight the different contributions of $\mathrm{Var}(M^1)$, it is useful to compare the considered model with a static population of compartments, where both the intake rate k_I and the exit rate k_E are set to zero. In the latter case, the number of compartments stays constant at the initial value $N(0) = N_0$, but the chemical birth-death events keep occurring independently in each compartment with rates k_b and k_d. For compactness, we will refer to this situation as "fixed population", whereas "dynamic population" refers to the full model with non-zero intake- and exit rates.

In Fig. S.1, we compare the expected total mass dynamics of a fixed population comprising $N_0 = 100$ empty compartments with that of a dynamic population for different choices of intake parameter. The dynamic case corresponds to compartment rates $k_I = 1$ and $k_E = 0.01$ and is initialized with one empty compartment. To allow for a meaningful comparison, the average steady-state number of compartments in the dynamic population was chosen to match the number of compartments in the fixed population, i.e., $\langle N_\infty\rangle = k_I/k_E = 100 = N_0$. The convergence towards steady state of the expected total mass $\langle M^1\rangle$ is slower in the dynamic scenario because it is limited by the rate at which compartments populate the system. More precisely, the slowest time scale is set by $1/k_E = 100$ in the dynamic case, while in the fixed case it is governed by the inverse of the degradation rate $1/k_d = 10$.

For all considered values of β, Fig. S.1 shows that the compartment fluctuations of the dynamic case produce a significantly larger variance $\mathrm{Var}(M^1_\infty)$ with respect to the fixed case, where only molecular noise is present. Next, we analyse the noise contributions to $\mathrm{Var}(M^1_\infty)$ for the Poissonian case $\beta = 1$, illustrated in the central panel of Fig. S.1. This is especially suitable because the expected total mass of dynamic- and fixed scenario coincide by construction. The mass variance of the fixed population is readily obtained by

$$\sigma^2_{\mathrm{fix}} = \mathrm{Var}\left(\sum_{i=1}^{N_0} X_\infty\right) = N_0 \mathrm{Var}(X_\infty) = N_0 \frac{k_d}{k_b}, \tag{S.7.41}$$

where the steady-state compartment content X_∞ is Poisson distributed with mean k_b/k_d. From the steady-state solution of the moment equations, it is possible to obtain a compact expression for $\mathrm{Var}(M^1_\infty)$ also in the dynamic scenario for the choice $\beta = 1$. We recall that, in these settings, the intake distribution $\pi_{Poiss}(x; \lambda = k_b/k_d)$ matches the steady-state realized by the chemical reactions, thereby leaving the Poisson distribution of X_∞ unaffected. Given that the number dynamics is independent of the compartment contents in this model, it follows that $\mathrm{Var}(M^1_\infty)$ can be identified as the variance of a compound Poisson process

$$\begin{aligned}\sigma^2_{\mathrm{dyn}} &= \mathrm{Var}\left(\sum_{i=1}^{N_\infty} X_\infty\right) = \langle N_\infty\rangle \mathrm{Var}(X_\infty) + \mathrm{Var}(N_\infty)\langle X_\infty\rangle^2 \\ &= \langle N_\infty\rangle \frac{k_b}{k_d} + \langle N_\infty\rangle \left(\frac{k_b}{k_d}\right)^2 = \langle N_\infty\rangle \langle X^2_\infty\rangle,\end{aligned} \tag{S.7.42}$$

where we used the law of total variance and result S.7.26. Comparing the first line of eq. S.7.42 with the fixed case S.7.41, we observe the presence of the additional term $\mathrm{Var}(N_\infty)\langle X_\infty\rangle^2$, which stems from the fluctuations of the compartment number at steady state. As a consequence of Poissonian statistics, we recognize that $\sigma^2_{\mathrm{dyn}}/\sigma^2_{\mathrm{fix}} = 1 + k_b/k_d = 1 + 10 = 11$. This analysis

shows that compartment events account for the majority of the mass variance, with a ratio of 10 to 1 in comparison to chemical events for the chosen parameter settings. This value is confirmed by analysing the standard deviations observed in the central panel of Fig. S.1, which exhibit a ratio equal to $\sqrt{11} \approx 3.31$.

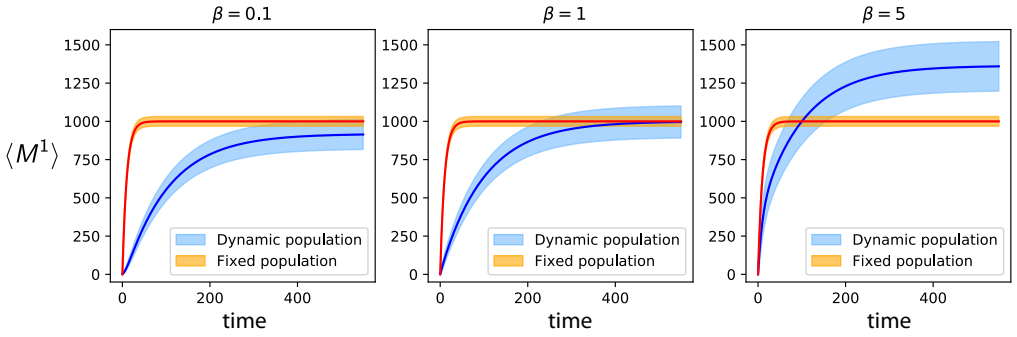

Figure S.1: Comparison of the expected total mass dynamics of the nested birth-death model between a fixed compartment population and a dynamic compartment population, the latter for rescaled intake mean $\beta = \lambda/(k_b/k_d)$ varied as indicated in the three panels. The fixed scenario corresponds to compartment intake and exit rates set to zero ($k_I = k_E = 0$), while the dynamic scenario corresponds to the choice $k_I = 1$ and $k_E = 0.01$. In all panels and for both scenarios, the birth-death parameters are set to $k_b = 1$ and $k_d = 0.1$. The fixed-population is initialized with $N_0 = 100$ empty compartments and the dynamic one with $N(0) = 1$ empty compartment. Solid lines and shaded areas represent the average dynamics surrounded above and below by one standard deviation. The results were obtained with moment equations.

S.8 CASE STUDY: Stochastic model of a coagulation-fragmentation process

This case study is defined by the transition classes

$$\begin{aligned}
\emptyset &\xrightarrow{h_I(\mathbf{n};y)} [y] && h_I(\mathbf{n};y) = k_I \pi_{Poiss}(y;\lambda) \\
[x] &\xrightarrow{h_E(\mathbf{n};x)} \emptyset && h_E(\mathbf{n};x) = k_E n(x) \\
[x] + [x'] &\xrightarrow{h_C(\mathbf{n};x,x')} [x+x'] && h_C(\mathbf{n};x,x') = k_C \frac{n(x)(n(x') - \delta_{x,x'})}{1+\delta_{x,x'}} \\
[x] &\xrightarrow{h_F(\mathbf{n};x,y)} [y] + [x-y] && h_F(\mathbf{n};x,y) = k_F x n(x) \pi_F(y|x).
\end{aligned} \tag{S.8.43}$$

Since the first two classes are equivalent to the previous case study, we will focus explicitly on the treatment of the coagulation and fragmentation transitions.

S.8.1 Moment equations

The total propensity of the random-coagulation class is found to be

$$H_C(\mathbf{n}) = \sum_{x=0}^{\infty} \sum_{x'=0}^{\infty} k_C \frac{n(x)(n(x') - \delta_{x,x'})}{2} = k_C \frac{N(N-1)}{2}, \tag{S.8.44}$$

where the factor $1/2$ accounts for double counting in the case $x \neq x'$ and arises from the binomial $\binom{n(x)}{2}$ for $x = x'$. We find that the total propensity is equal to the coagulation rate k_C multiplied by the number of distinct compartment pairs $\binom{N}{2}$, which is consistent with a random coagulation mechanism.

We recall that the fragmentation transition class is in general defined as

$$[\mathbf{x}] \xrightarrow{h_F(\mathbf{n};\mathbf{x},\mathbf{y})} [\mathbf{y}] + [\mathbf{x}-\mathbf{y}], \tag{S.8.45}$$

where we have already substituted the mass-conservation constraint in the right-hand side. The corresponding propensity function is

$$h_F(\mathbf{n};\mathbf{x},\mathbf{y}) = k_F g_F(\mathbf{x}) n(\mathbf{x}) \pi_F(\mathbf{y}|\mathbf{x}). \tag{S.8.46}$$

Note that $g_F(\mathbf{x})$ controls the probability of the "mother" compartment to undergo a fragmentation event. The probability distribution $\pi_F(\mathbf{y}|\mathbf{x})$ expresses the probability that one of the two fragments has a content equal to $\mathbf{y}$. The distribution $\pi_F(\mathbf{y}|\mathbf{x})$ must be symmetric with respect to $\mathbf{y}$ and $\mathbf{x}-\mathbf{y}$. In this example, the compartment content is one-dimensional (i.e. $\mathbf{x} = x$), we choose $g_F(x) = x$ and for $\pi_F(\mathbf{y}|\mathbf{x})$ a uniform fragment distribution

$$\pi_F(y|x) = \frac{1}{x+1} \quad \text{with} \quad 0 \le y \le x, \tag{S.8.47}$$

which permits the creation of empty daughter compartments too. The corresponding total fragmentation propensity is equal to

$$\begin{aligned} H_F(\mathbf{n}) &= \sum_{x=0}^{\infty} \sum_{y=0}^{x} k_F g_F(x) n(x) \pi_F(y|x) \\ &= k_F \sum_{x=0}^{\infty} x n(x) \sum_{y=0}^{x} \pi_F(y|x) = k_F M^1. \end{aligned} \tag{S.8.48}$$

The moment equations for this model read

$$\begin{aligned} \frac{\mathrm{d}\langle N\rangle}{\mathrm{d}t} &= k_I - k_E\langle N\rangle - \frac{k_C}{2}\big(\langle N^2\rangle - \langle N\rangle\big) + k_F\langle M^1\rangle \\ \frac{\mathrm{d}\langle N^2\rangle}{\mathrm{d}t} &= k_I(1 + 2\langle N\rangle) + k_E\big(\langle N\rangle - 2\langle N^2\rangle\big) + \frac{k_C}{2}\big(\langle N^2\rangle - \langle N\rangle\big) - k_C\big(\langle N^3\rangle - \langle N^2\rangle\big) \\ &\quad + k_F\big(\langle M^1\rangle + 2\langle NM^1\rangle\big) \\ \frac{\mathrm{d}\langle M^1\rangle}{\mathrm{d}t} &= k_I\lambda - k_E\langle M^1\rangle \\ \frac{\mathrm{d}\langle (M^1)^2\rangle}{\mathrm{d}t} &= k_I\lambda(1 + \lambda + 2\langle M^1\rangle) + k_E(\langle M^2\rangle - 2\langle (M^1)^2\rangle) \\ \frac{\mathrm{d}\langle M^2\rangle}{\mathrm{d}t} &= k_I\lambda(1+\lambda) - k_E\langle M^2\rangle + k_C\big(\langle (M^1)^2\rangle - \langle M^2\rangle\big) + \frac{k_F}{3}\big(\langle M^2\rangle - \langle M^3\rangle\big) \\ \frac{\mathrm{d}\langle NM^1\rangle}{\mathrm{d}t} &= k_I\big(\lambda(1 + \langle N\rangle) + \langle M^1\rangle\big) + k_E(\langle M^1\rangle - 2\langle NM^1\rangle) \\ &\quad + \frac{k_C}{2}\big(\langle NM^1\rangle - \langle N^2M^1\rangle\big) + k_F\langle (M^1)^2\rangle \end{aligned} \tag{S.8.49}$$

and we employ the Gamma closure scheme on the following third-order moments

$$\begin{aligned} \langle N^3\rangle &= 2\frac{\langle N^2\rangle^2}{\langle N\rangle} - \langle N^2\rangle\langle N\rangle \\ \langle N^2M^1\rangle &= 2\frac{\langle N^2\rangle\langle NM^1\rangle}{\langle N\rangle} - \langle N^2\rangle\langle M^1\rangle \\ \langle M^3\rangle &= 2\frac{\langle (M^2)\rangle^2}{\langle M^1\rangle} - \frac{\langle M^2\rangle\langle M^1\rangle}{\langle N\rangle}. \end{aligned} \tag{S.8.50}$$

Since the total mass M^1 is not affected by coagulation or fragmentation events, we find the equations for $\langle M^1\rangle$ and $\langle (M^1)^2\rangle$ to be identical to the previous case study in terms of intake and exit contributions. The derivation of the equations for $\langle N\rangle$ and $\langle N^2\rangle$ is also straightforward

and resembles closely the treatment of eqs. S.7.16 and S.7.17. Here we explicitly show only the derivation of the coagulation-fragmentation contributions of $\mathrm{d}\langle M^2\rangle/\mathrm{d}t$:

$$\begin{aligned}
\left.\frac{\mathrm{d}\langle M^2\rangle}{\mathrm{d}t}\right|_{C,F} &= \Big\langle \sum_{x=0}^{\infty}\sum_{x'=0}^{\infty}\big[(x+x')^2-(x)^2-(x')^2\big]k_C\frac{n(x)(n(x')-\delta_{x,x'})}{2}\Big\rangle \\
&\quad+\Big\langle \sum_{x=0}^{\infty}\sum_{y=0}^{x}\big[y^2+(x-y)^2-x^2\big]k_F x n(x)\pi_F(y|x)\Big\rangle \\
&= k_C\Big\langle \sum_{x=0}^{\infty}\sum_{x'=0}^{\infty}\big[2xx'\big]\frac{n(x)(n(x')-\delta_{x,x'})}{2}\Big\rangle \\
&\quad+k_F\Big\langle \sum_{x=0}^{\infty} x n(x)\sum_{y=0}^{x}2\big[y^2-xy\big]\pi_F(y|x)\Big\rangle \\
&= k_C\Big\langle \sum_{x=0}^{\infty} x n(x)\sum_{x'=0}^{\infty} x' n(x')\Big\rangle - k_C\Big\langle\sum_{x=0}^{\infty}x^2 n(x)\Big\rangle \\
&\quad+2k_F\Big\langle \sum_{x=0}^{\infty} x n(x)\Big[\frac{2x^2+x}{6}-x\frac{x}{2}\Big]\Big\rangle \\
&= k_C\big(\langle(M^1)^2\rangle-\langle M^2\rangle\big)+\frac{k_F}{3}\big(\langle M^2\rangle-\langle M^3\rangle\big).
\end{aligned} \tag{S.8.51}$$

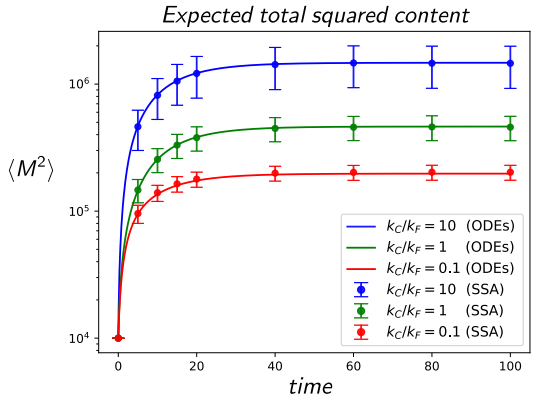

Figure S.2: Agreement of the expected dynamics of the second order moment $M^2 = \sum_{x=0}^{\infty} x^2 n(x)$ between the Gamma-closed moment equations (ODEs) and the estimate obtained from stochastic simulations (SSA). Dots and error bars represent the mean value and one standard deviation above and below the mean. The variability of $\langle M^2\rangle$ cannot be reported from the solution of the moment equations because the equation for $\langle(M^2)^2\rangle$ was not included.

S.8.2 Simulation parameters

In Figures 2E-F in the main paper we used the following choice of parameters

$$k_I = 10 \qquad \lambda = 50 \qquad k_E = 0.1 \qquad k_F = 5\cdot 10^{-3}$$

and k_C takes the values $[0.1k_F, k_F, 10k_F]$ in the three cases. The initial condition was set to

$$\mathbf{n}_0 : n_0(10) = 100,\ \ n_0(x) = 0\ \ \forall x \neq 10$$

which represents a population comprising 100 compartments with content $x = 10$. Monte Carlo estimates have been obtained by averaging the outputs of 10^4 stochastic simulations, for each parameter combination. In Fig. S.2 we show the accuracy of the solution for $\langle M^2\rangle$ obtained in these settings, next to the estimate from exact stochastic simulations.

S.9 CASE STUDY: Protein expression dynamics in a cell community

The state space of the compartment content (x_G, x_P) is $\mathbb{X} = [0,1]\times\mathbb{N}_0$, where $x_G = 1$ represents the binary gene variable in the active state. The protein expression network in each cell is modelled as

$$\begin{aligned}
[x_G, x_P] &\xrightarrow{h_b^G(\mathbf{n};\mathbf{x})} [1, x_P] && h_b^G(\mathbf{n};\mathbf{x}) = k_b^G(1-x_G)n(\mathbf{x}) \\
[x_G, x_P] &\xrightarrow{h_d^G(\mathbf{n};\mathbf{x})} [0, x_P] && h_d^G(\mathbf{n};\mathbf{x}) = k_d^G x_G n(\mathbf{x}) \\
[x_G, x_P] &\xrightarrow{h_P(\mathbf{n};\mathbf{x})} [x_G, x_P+1] && h_P(\mathbf{n};\mathbf{x}) = k_P x_G n(\mathbf{x}) \\
[x_G, x_P] &\xrightarrow{h_d^P(\mathbf{n};\mathbf{x})} [x_G, x_P-1] && h_d^P(\mathbf{n};\mathbf{x}) = k_d^P x_P n(\mathbf{x}).
\end{aligned} \tag{S.9.52}$$

The communication class for which active cells can induce activation in inactive cells is defined by

$$[\mathbf{x}] + [\mathbf{x}'] \xrightarrow{h_{\text{com}}(\mathbf{n};\mathbf{x},\mathbf{x}')} [1, x_P] + [1, x'_P] \tag{S.9.53}$$

where

$$\begin{aligned}
h_{\text{com}}(\mathbf{n};\mathbf{x},\mathbf{x}') &= k_{\text{com}} g_{\text{com}}(\mathbf{x},\mathbf{x}') \frac{n(\mathbf{x})(n(\mathbf{x}') - \delta_{\mathbf{x},\mathbf{x}'})}{1+\delta_{\mathbf{x},\mathbf{x}'}} \\
\text{with } g_{\text{com}}(\mathbf{x},\mathbf{x}') &= x_G(1-x'_G) + x'_G(1-x_G).
\end{aligned} \tag{S.9.54}$$

The content-dependent function g_{com} ensures the transition to happen only between an active and inactive cell. This expression for g_{com} also implies that the cell-cell activation happens with equal probability among any active or inactive cell, irrespectively of their protein content, since there is no explicit dependency on x_P and x'_P.

S.9.1 Moment equations

The total propensity of the cell communication class is found to be

$$\begin{aligned}
H_{\text{com}}(\mathbf{n}) &= \sum_{\mathbf{x}}\sum_{\mathbf{x}'} k_{\text{com}}\big(x_G(1-x'_G) + x'_G(1-x_G)\big)\frac{n(\mathbf{x})(n(\mathbf{x}')-\delta_{\mathbf{x},\mathbf{x}'})}{2} \\
&= \frac{k_{\text{com}}}{2}\sum_{\mathbf{x}}\sum_{\mathbf{x}'}\big(x_G + x'_G - 2x_G x'_G\big)n(\mathbf{x})n\big(\mathbf{x}'\big) - \frac{k_{\text{com}}}{2}\sum_{\mathbf{x}}\big(2x_G - 2x_G^2\big)n(\mathbf{x}) \\
&= \frac{k_{\text{com}}}{2}\left(\sum_{\mathbf{x}} x_G n(\mathbf{x})\sum_{\mathbf{x}'} n\big(\mathbf{x}'\big) + \sum_{\mathbf{x}} n(\mathbf{x})\sum_{\mathbf{x}'} x'_G n\big(\mathbf{x}'\big)\right) \\
&\quad - k_{\text{com}}\sum_{\mathbf{x}} x_G n(\mathbf{x})\sum_{\mathbf{x}'} x'_G n\big(\mathbf{x}'\big) \\
&= k_{\text{com}}\big(NM^{1,0} - (M^{1,0})^2\big) \\
&= k_{\text{com}} M^{1,0}\big(N_0 - M^{1,0}\big),
\end{aligned} \tag{S.9.55}$$

where from the second to third line we have made use of the fact that $x_G = x_G^2$, since $x_G \in [0,1]$. The factor $1/2$ in the propensity function originates in the same way as in the calculation of S.8.44. As expected, the total communication propensity equals the rate k_{com} times the product of the number of active and inactive cells.

The system of moment equations describing the evolution of this model is

$$
\begin{aligned}
\frac{\mathrm{d}\langle M^{1,0}\rangle}{\mathrm{d}t} &= k_{\mathrm{com}}\big(N_0\langle M^{1,0}\rangle - \langle (M^{1,0})^2\rangle\big) + k_b^G\big(N_0 - \langle M^{1,0}\rangle\big) - k_d^G\langle M^{1,0}\rangle \\
\frac{\mathrm{d}\langle (M^{1,0})^2\rangle}{\mathrm{d}t} &= k_{\mathrm{com}}\big(N_0\langle M^{1,0}\rangle - \langle (M^{1,0})^2\rangle\big) + 2k_{\mathrm{com}}\big(N_0\langle (M^{1,0})^2\rangle - \langle (M^{1,0})^3\rangle\big) \\
&\quad + k_b^G\big[N_0 - \langle M^{1,0}\rangle + 2\big(N_0\langle M^{1,0}\rangle - \langle (M^{1,0})^2\rangle\big)\big] \\
&\quad + k_d^G\big(\langle M^{1,0}\rangle - 2\langle (M^{1,0})^2\rangle\big) \\
\frac{\mathrm{d}\langle M^{0,1}\rangle}{\mathrm{d}t} &= k_P\langle M^{1,0}\rangle - k_d^P\langle M^{0,1}\rangle \\
\frac{\mathrm{d}\langle (M^{0,1})^2\rangle}{\mathrm{d}t} &= k_P\big(\langle M^{1,0}\rangle + 2\langle M^{1,0}M^{0,1}\rangle\big) + k_d^P\big(\langle M^{0,1}\rangle - 2\langle (M^{0,1})^2\rangle\big) \\
\frac{\mathrm{d}\langle M^{1,0}M^{0,1}\rangle}{\mathrm{d}t} &= k_{\mathrm{com}}\big(N_0\langle M^{1,0}M^{0,1}\rangle - \langle (M^{1,0})^2M^{0,1}\rangle\big) + k_P\langle (M^{1,0})^2\rangle \\
&\quad + k_b^G\big(N_0\langle M^{0,1}\rangle - \langle M^{1,0}M^{0,1}\rangle\big) - \Big(k_d^G + k_d^P\Big)\langle M^{1,0}M^{0,1}\rangle
\end{aligned}
\tag{S.9.56}
$$

and we employ the Gamma closure scheme on the following third-order moments:

$$
\begin{aligned}
\langle (M^{1,0})^3\rangle &= 2\frac{\langle (M^{1,0})^2\rangle^2}{\langle M^{1,0}\rangle} - \langle (M^{1,0})^2\rangle\langle M^{1,0}\rangle \\
\langle (M^{1,0})^2M^{0,1}\rangle &= 2\frac{\langle (M^{1,0})^2\rangle\langle M^{1,0}M^{0,1}\rangle}{\langle M^{1,0}\rangle} - \langle (M^{1,0})^2\rangle\langle M^{0,1}\rangle.
\end{aligned}
\tag{S.9.57}
$$

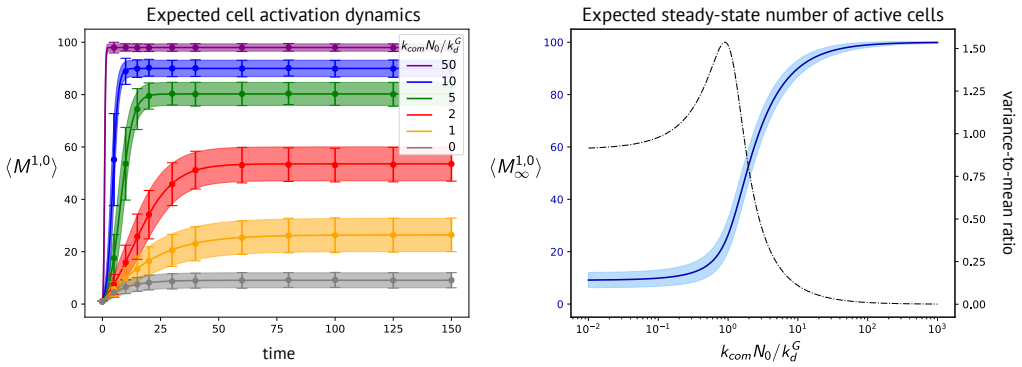

Figure S.3: On the left, the expected dynamics of the number of active cells $M^{1,0}$ and its variability for different values of the communication rate. Results from moment equations are shown in solid lines and shaded areas, and estimates from stochastic simulation in dots and error bars. The mean value is surrounded above and below by one standard deviation. On the right, the expected steady-state number of active cells is plotted as a function of the rescaled communication rate $k_{\mathrm{com}}N_0/k_d^G$. The dashed-dotted black line shows the variance-to-mean ratio, computed as $\mathrm{Var}(M_\infty^{1,0})/\langle M_\infty^{1,0}\rangle$ from moment equations.

S.9.2 Simulation parameters

In Figures 3B-C in the main paper we used for the following choice of parameters

$$
k_b^G = 0.01 \qquad k_d^G = 0.1 \qquad k_P = 1 \qquad k_d^P = 0.05
$$

and k_{com} takes the values $[0, 10^{-3}, 2\cdot 10^{-3}, 5\cdot 10^{-3}, 10^{-2}, 5\cdot 10^{-2}]$. The initial condition was set to

$$
\mathbf{n}_0 : n_0([1,1]) = 1, \;\; n_0(\mathbf{0}) = 99,
$$

which represents a population comprising 100 cells, one of which is in active state and contains one protein molecule and the remaining 99 are in inactive state and with empty content. Monte Carlo estimates have been obtained by averaging the outputs of 10^3 stochastic simulations, for each parameter combination. In Fig. S.3 we report the expected cell activation dynamics across the cell population, which complements Figs. 3B,C of the main paper.

S.10 CASE STUDY: Stem cell population dynamics

Also in this case study, the state space of the compartment content $\mathbf{x} = (x_G, x_S)$ is $\mathbb{X} = [0,1] \times \mathbb{N}_0$, where $x_G = 1$ indicates a stem cell and $x_G = 0$ a differentiated cell. The considered transition classes are

$$\begin{aligned}
&[\mathbf{x}] \xrightarrow{h_F^+(\mathbf{n};\mathbf{x})} [x_G, 0] + [x_G, 0] && h_F^+(\mathbf{n};\mathbf{x}) = k_F^+ x_G x_S n(\mathbf{x}) \\
&[\mathbf{x}] \xrightarrow{h_F^-(\mathbf{n};\mathbf{x})} [x_G, 0] + [1 - x_G, 0] && h_F^-(\mathbf{n};\mathbf{x}) = k_F^- x_G x_S n(\mathbf{x}) \\
&[\mathbf{x}] \xrightarrow{h_S(\mathbf{n};\mathbf{x})} [x_G, x_S + 1] && h_S(\mathbf{n};\mathbf{x}) = k_S x_G n(\mathbf{x}) \\
&[\mathbf{x}] \xrightarrow{h_E(\mathbf{n};\mathbf{x})} \emptyset && h_E(\mathbf{n};\mathbf{x}) = k_E(1 - x_G) n(\mathbf{x}) \\
&[\mathbf{x}] + [\mathbf{x}'] \xrightarrow{h_{\mathrm{nf}}(\mathbf{n};\mathbf{x},\mathbf{x}',\mathbf{y},\mathbf{y}')} [\mathbf{y}] + [\mathbf{y}']
\end{aligned} \tag{S.10.58}$$

with

$$h_{\mathrm{nf}}(\mathbf{n};\mathbf{x},\mathbf{x}',\mathbf{y},\mathbf{y}') = k_{\mathrm{nf}} x_G x'_G \frac{n(\mathbf{x})(n(\mathbf{x}') - \delta_{\mathbf{x},\mathbf{x}'})}{1 + \delta_{\mathbf{x},\mathbf{x}'}} \pi_{\mathrm{nf}}(\mathbf{y},\mathbf{y}' \mid \mathbf{x},\mathbf{x}') \tag{S.10.59}$$

and outcome distribution is given by

$$\pi_{\mathrm{nf}}(\mathbf{y},\mathbf{y}' \mid \mathbf{x},\mathbf{x}') = \begin{cases} \frac{1}{2} & \text{if } \mathbf{y} = \mathbf{x},\ y'_G = 1 - x'_G,\ y'_S = x'_S \\ \frac{1}{2} & \text{if } \mathbf{y}' = \mathbf{x}',\ y_G = 1 - x_G,\ y_S = x_S \\ 0 & \text{else.} \end{cases} \tag{S.10.60}$$

The negative-feedback mechanism encoded by the propensity of eq. S.10.59 can be understood as follows: first, two stem cells are randomly selected from the current state $\mathbf{n}$, as enforced by the choice $g_{\mathrm{nf}}(\mathbf{x},\mathbf{x}') = x_G x'_G$. Then, one of the two stem cells is randomly differentiated by switching x_G to zero, as encoded by π_{nf}. Note that the x_G-dependence of the propensity functions determines the selectivity for either stem cells or differentiated cells also for the remaining transition classes. For instance, the division events can occur only to stem cells, since their propensities h_F^+ and h_F^- would be zero when the reactant cell is a differentiated cell (i.e. $x_G = 0$). The same is true for h_S. Conversely, the death event applies only to differentiated cells, since $h_E(\mathbf{n};\mathbf{x}) = 0$ for stem cells.

Next, we show the computation of the total class propensity for the feedback transition class. The latter is given by

$$\begin{aligned}
H_{\mathrm{nf}}(\mathbf{n}) &= \sum_{\mathbf{x},\mathbf{x}'} k_{\mathrm{nf}} x_G x'_G \frac{n(\mathbf{x})(n(\mathbf{x}') - \delta_{\mathbf{x},\mathbf{x}'})}{2} \\
&= \frac{k_{\mathrm{nf}}}{2} \left(\sum_{\mathbf{x}} x_G n(\mathbf{x}) \sum_{\mathbf{x}'} x'_G n(\mathbf{x}') - \sum_{\mathbf{x}} x_G n(\mathbf{x}) \right) \\
&= k_{\mathrm{nf}} \frac{M^{1,0}(M^{1,0} - 1)}{2} = k_{\mathrm{nf}} \binom{M^{1,0}}{2},
\end{aligned} \tag{S.10.61}$$

where the binomial factor reflects that the negative feedback acts between randomly chosen pairs of stem cells. In particular, the factor $1/2$ appearing in the first line of eq. S.10.61 originates from π_{nf} whenever $\mathbf{x} \neq \mathbf{x}'$ and from the binomial factor of eq. S.10.59 when $\mathbf{x} = \mathbf{x}'$, in which case π_{nf} gives only one distinguishable outcome and thus contributes with value 1.

The total propensities for the remaining transition classes of the model are readily computed:

$$\begin{aligned} H_F^+(\mathbf{n}) &= k_F^+ M^{1,1} \\ H_F^-(\mathbf{n}) &= k_F^- M^{1,1} \\ H_S(\mathbf{n}) &= k_S M^{1,0} \\ H_E(\mathbf{n}) &= k_E\big(N - M^{1,0}\big) \end{aligned} \tag{S.10.62}$$

S.10.1 Moment equations

Due to the combined presence of the moment $M^{1,1}$ and the structure of the feedback class, the derivation of a closed set of moment equations is more challenging than for the previous models. This is why we focus on deriving equations for moments directly entering in the total class propensities, and at the same time to avoid further equations for less relevant population statistics which would introduce additional higher order dependencies. From eq. S.10.61 and S.10.62 we see that, together with $M^{1,1}$, the overall dynamics is also governed by the total number of cells N and the number of stem cells $M^{1,0}$. The SDEs for these moments are given by

$$\begin{aligned} \mathrm{d}N &= \sum_{\mathbf{x}} \big(\mathrm{d}R^+_{F,\mathbf{x}} + \mathrm{d}R^-_{F,\mathbf{x}} - \mathrm{d}R_{E,\mathbf{x}}\big) = \mathrm{d}\bar{R}^+_F + \mathrm{d}\bar{R}^-_F - \mathrm{d}\bar{R}_E \\ \mathrm{d}M^{1,0} &= \sum_{\mathbf{x}} \mathrm{d}R^+_{F,\mathbf{x}} - \sum_{\mathbf{x}}\sum_{\mathbf{x}'} \mathrm{d}R_{\mathrm{nf},\mathbf{x},\mathbf{x}'} = \mathrm{d}\bar{R}^+_F - \mathrm{d}\bar{R}_{\mathrm{nf}} \\ \mathrm{d}M^{1,1} &= \sum_{\mathbf{x}} \mathrm{d}R_{S,\mathbf{x}} - \sum_{\mathbf{x}} x_S\big(\mathrm{d}R^+_{F,\mathbf{x}} + \mathrm{d}R^-_{F,\mathbf{x}}\big) - \sum_{\mathbf{x}}\sum_{\mathbf{x}'} x_S \mathrm{d}R_{\mathrm{nf},\mathbf{x},\mathbf{x}'}, \end{aligned} \tag{S.10.63}$$

where the enumeration of single transitions spans $\mathbb{X}$ for all transition classes with exception of the feedback, where all distinguishable transitions can be written as the iteration over $\mathbf{x}, \mathbf{x}' \in \mathbb{X}^2$ and where $\mathbf{x}$ denotes the content of the cell which differentiates. The first two equations have been rewritten also in terms of the class reaction counters, which better highlight their meaning. We see how the total number of cells increases by 1 whenever a division event occurs and decreases by 1 in occurrence of the death of any differentiated cell. On the other hand, the number of stem cells $M^{1,0}$ is increased by 1 only when a symmetric division occurs, and is decreased by 1 as a result of a feedback conversion. On the opposite, $M^{1,0}$ is left unaffected by asymmetric divisions.

After taking expectations of S.10.63 and including further equations for some direct moment dependencies, we obtain the following set of moment equations

$$\begin{aligned} \frac{\mathrm{d}\langle N\rangle}{\mathrm{d}t} &= \big(k_F^+ + k_F^-\big)\langle M^{1,1}\rangle - k_E\big(\langle N\rangle - \langle M^{1,0}\rangle\big) \\ \frac{\mathrm{d}\langle N^2\rangle}{\mathrm{d}t} &= \big(k_F^+ + k_F^-\big)\big(\langle M^{1,1}\rangle + 2\langle NM^{1,1}\rangle\big) + k_E\big[\langle N\rangle - \langle M^{1,0}\rangle - 2\big(\langle N^2\rangle - \langle NM^{1,0}\rangle\big)\big] \\ \frac{\mathrm{d}\langle M^{1,0}\rangle}{\mathrm{d}t} &= k_F^+\langle M^{1,1}\rangle - k_{\mathrm{nf}}\frac{\langle (M^{1,0})^2\rangle - \langle M^{1,0}\rangle}{2} \\ \frac{\mathrm{d}\langle (M^{1,0})^2\rangle}{\mathrm{d}t} &= k_F^+\big(\langle M^{1,1}\rangle + 2\langle M^{1,0}M^{1,1}\rangle\big) \\ &\quad + k_{\mathrm{nf}}\frac{\langle (M^{1,0})^2\rangle - \langle M^{1,0}\rangle}{2} - k_{\mathrm{nf}}\big(\langle (M^{1,0})^3\rangle - \langle (M^{1,0})^2\rangle\big) \\ \frac{\mathrm{d}\langle M^{1,1}\rangle}{\mathrm{d}t} &= k_S\langle M^{1,0}\rangle - \big(k_F^+ + k_F^-\big)\langle M^{1,2}\rangle - k_{\mathrm{nf}}\frac{\langle M^{1,0}M^{1,1}\rangle - \langle M^{1,1}\rangle}{2} \\ \frac{\mathrm{d}\langle M^{1,2}\rangle}{\mathrm{d}t} &= k_S\big(\langle M^{1,0}\rangle + 2\langle M^{1,1}\rangle\big) - \big(k_F^+ + k_F^-\big)\langle M^{1,3}\rangle - k_{\mathrm{nf}}\frac{\langle M^{1,0}M^{1,2}\rangle - \langle M^{1,2}\rangle}{2} \end{aligned} \tag{S.10.64}$$

and we employ the Gamma closure scheme

$$\begin{aligned} \langle (M^{1,0})^3\rangle &= 2\frac{\langle (M^{1,0})^2\rangle^2}{\langle M^{1,0}\rangle} - \langle (M^{1,0})^2\rangle\langle M^{1,0}\rangle \\ \langle M^{1,3}\rangle &= 2\frac{\langle (M^{1,2})^2\rangle^2}{\langle M^{1,1}\rangle} - \frac{\langle M^{1,2}\rangle\langle M^{1,1}\rangle}{\langle M^{1,0}\rangle}. \end{aligned} \tag{S.10.65}$$

For the remaining cross-moments, we use a mean-field approximation. This is understood as the following substitution

$$\langle M^\gamma M^\xi \rangle = \langle M^\gamma \rangle \langle M^\xi \rangle, \tag{S.10.66}$$

which means to neglect the correlation between the two moments M^γ and M^ξ. We applied the mean-field approximation on $\langle NM^{1,0} \rangle$, $\langle NM^{1,1} \rangle$, $\langle M^{1,0} M^{1,1} \rangle$ and $\langle M^{1,0} M^{1,2} \rangle$. In this example, one of the effects of such simplification seems to be noticeable from the expected fluctuations of N and $M^{1,0}$ in Fig. 3F: the variability predicted by moment equations is smaller than the error bars obtained by exact stochastic simulations.

S.10.2 Simulation parameters

Figures 3E-F and the parameter reference for figures 3G-H in the main paper correspond to the following choice of parameters

$$k_F^+ = k_F^- = 5 \cdot 10^{-3} \qquad k_S = 10 \qquad k_E = 0.05 \qquad k_{\text{nf}} = 0.01$$

The two initial conditions of Fig. 3F are

$$\mathbf{n}_0 : n_0([1,1]) = 1, \;\; n_0(\mathbf{x}) = 0 \;\; \forall \mathbf{x} \neq [1,1]$$

and

$$\mathbf{n}_0 : n_0([1,1]) = 100, \;\; n_0(\mathbf{x}) = 0 \;\; \forall \mathbf{x} \neq [1,1],$$

which represent a population made either of one or 100 stem cells, each having $x_S = 1$. Monte Carlo estimates have been obtained by averaging the outputs of 10^3 stochastic simulations.

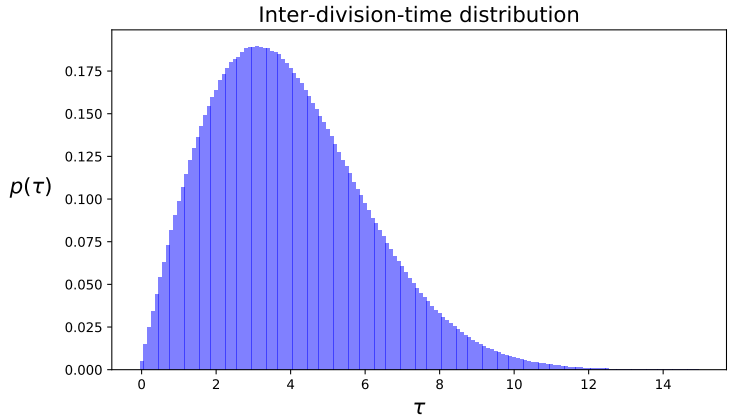

Figure S.4: Empirical distribution of the waiting-time τ until cell division, computed with stochastic simulations. This corresponds to a model where the cell-cycle factor x_S follows a birth process of rate k_S and cell division occurs with rate $k_F x_S$. The parameters have been set to $k_S = 10$ and $k_F = k_F^+ + k_F^- = 0.01$, in line with the choice reported in section S.10.2.

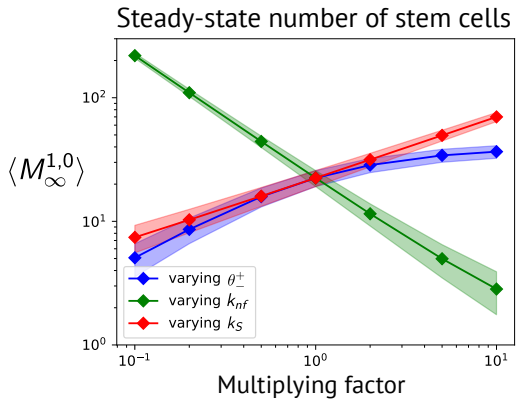

Figure S.5: Steady-state number of stem cells upon variations of different parameters, obtained from moment equations. The mean value is surrounded above and below by one standard deviation. The reference parameter values correspond to the choice provided in section S.10.2.

References

[1] P. K. Andersen, O. Borgan, R. D. Gill, and N. Keiding, *Statistical models based on counting processes*. Springer Science & Business Media, 2012.

[2] B. Øksendal and A. Sulem, *Applied stochastic control of jump diffusions*. Springer Science & Business Media, 2007.

[3] D. Schnoerr, G. Sanguinetti, and R. Grima, "Validity conditions for moment closure approximations in stochastic chemical kinetics," *The Journal of Chemical Physics*, vol. 141, no. 8, p. 084103, 2014.

[4] E. Lakatos, A. Ale, P. D. W. Kirk, and M. P. H. Stumpf, "Multivariate moment closure techniques for stochastic kinetic models," *The Journal of Chemical Physics*, vol. 143, no. 9, p. 094107, 2015.

[5] C. W. Gardiner *et al.*, *Handbook of stochastic methods*, vol. 3. Springer Berlin, 1985.